

Single crystal growth of the pyrochlores $R_2\text{Ti}_2\text{O}_7$ ($R =$ rare earth) by the optical floating-zone method

Q. J. Li, L. M. Xu, C. Fan, F. B. Zhang, Y. Y. Lv, B. Ni, Z. Y. Zhao, X. F. Sun*

Hefei National Laboratory for Physical Sciences at Microscale, University of Science and Technology of China, Hefei, Anhui 230026, China

Abstract

We report a systematic study on the crystal growth of the rare-earth titanates $R_2\text{Ti}_2\text{O}_7$ ($R =$ Gd, Tb, Dy, Ho, Y, Er, Yb and Lu) and Y-doped $\text{Tb}_{2-x}\text{Y}_x\text{Ti}_2\text{O}_7$ ($x = 0.2$ and 1) using an optical floating-zone method. High-quality single crystals were successfully obtained and the growth conditions were carefully optimized. The oxygen pressure was found to be the most important parameter and the appropriate ones are 0.1–0.4 MPa, depending on the radius of rare-earth ions. The growth rate is another parameter and was found to be 2.5–4 mm/h for different rare-earth ions. X-ray diffraction data demonstrated the good crystallinity of these crystals. The basic physical properties of these crystals were characterized by the magnetic susceptibility and specific heat measurements.

Keywords:

A2. Floating Zone technique, A2. Single crystal growth, A1. Characterization, B2. Magnetic materials

*Corresponding author. Tel.: 86-551-63600499, Fax: 86-551-63600499.
Email address: xfsun@ustc.edu.cn

1. Introduction

The rare-earth titanate with the pyrochlore structure, $R_2\text{Ti}_2\text{O}_7$ ($R =$ rare earth), crystallizes into a face centered cubic structure with eight formula units in a unit cell, and the space group is $Fd\bar{3}m$. The rare earth ions form a network of corner-sharing tetrahedra, of which the vertices are occupied by R^{3+} , with triangular and kagomé planes alternately stacked along the [111] direction. Recently, these materials have attracted considerable interests because of their three-dimensional feature of geometrical magnetic frustration and the resulting exotic ground states at low temperatures, including spin ice, spin liquid and order-by-disorder [1, 2, 3, 4]. Since these low-temperature magnetic properties are sometimes very sensitive to the sample quality, as was observed in $\text{Yb}_2\text{Ti}_2\text{O}_7$ and $\text{Tb}_2\text{Ti}_2\text{O}_7$ [5, 6], the growth of high-quality $R_2\text{Ti}_2\text{O}_7$ single crystals is very important for investigating the intrinsic physics of these materials. Both the flux method and the optical floating-zone technique have been tried for growing $R_2\text{Ti}_2\text{O}_7$ single crystals and the latter was found to be able to produce better and bigger crystals [7, 8, 10, 11, 12]. However, the detailed growing conditions of $R_2\text{Ti}_2\text{O}_7$ using the floating-zone method have not been systemically studied or reported and the crystal quality demonstrated in the literature seems to have significant room to improve.

In this work, we studied in details the conditions for the crystal growth of the $R_2\text{Ti}_2\text{O}_7$ ($R =$ Gd, Tb, Dy, Ho, Y, Er, Yb and Lu) using the floating-zone method. It was found that the growth rate, atmosphere and oxygen pressure should be carefully adjusted to get high-quality single crystals and they differ from each other for different rare-earth ions. Moreover, to study the magnetic dilution effect of the spin liquid $\text{Tb}_2\text{Ti}_2\text{O}_7$, we have grown $\text{Tb}_{2-x}\text{Y}_x\text{Ti}_2\text{O}_7$ ($x = 0.2$ and 1) single crystals by replacing magnetic Tb^{3+} ions with nonmagnetic Y^{3+} ions. The obtained crystals were well characterized by X-ray diffraction, magnetic susceptibility and specific heat measurements.

2. Crystal Growth

Single crystals of $R_2\text{Ti}_2\text{O}_7$ ($R = \text{Gd}, \text{Tb}, \text{Dy}, \text{Ho}, \text{Y}, \text{Er}, \text{Yb}$ and Lu) and $\text{Tb}_{2-x}\text{Y}_x\text{Ti}_2\text{O}_7$ ($x = 0.2$ and 1) were grown using an optical floating-zone furnace with four 1000 W halogen lamps (Crystal System Incorporation, Japan). $\text{Dy}_2\text{Ti}_2\text{O}_7$ was chosen as a trial to find the optimum growth condition for pyrochlore titanates. There are some earlier reports that $\text{Dy}_2\text{Ti}_2\text{O}_7$ single crystals could be grown in different atmospheres (O_2 , $\text{Ar}+\text{O}_2$ or Ar) with different growth rates [8, 12]. We found that the quality of $\text{Dy}_2\text{Ti}_2\text{O}_7$ single crystals is quite sensitive to such growing conditions as oxygen pressure and growth rate. At the beginning, we tried the growth at a rate of 2.5 mm/h and in flowing oxygen with 0.3 MPa pressure, which can ensure a stable growing. The diameter of crystal is very uniform compared to that grown in air (ambient pressure) in an earlier report [8]. The single crystal bar is transparent with the color of amber and develops small facets. However, it has some small cracks at the end part, as shown in Fig. 1(a), indicating that the growth condition is still not appropriate. Then, we tried to increase the oxygen pressure to 0.4 MPa and grew it with a rate of 2 mm/h, in which case the molten zone could not be stabilized and it dropped when the crystal growth has been continued for only 3–4 hours. A possible improving way is to change the growth rate. After several attempts, we finally got the optimum condition of 0.4 MPa oxygen pressure and 4 mm/h rate for $\text{Dy}_2\text{Ti}_2\text{O}_7$. As shown in Fig. 1(b), the as-grown single crystal displays a nice morphology, long consecutive facets and a homogenous amber color. The powder X-ray diffraction measured on a randomly selected part of $\text{Dy}_2\text{Ti}_2\text{O}_7$ single crystal confirmed the pure and single phase. In addition, a narrow width of the rocking curve of the (440) Bragg peak (FWHM $\approx 0.11^\circ$), as shown in Fig. 2, demonstrates that the crystal has good crystallinity. Therefore, the appropriate oxygen pressure and growth rate play important roles in the growth of $\text{Dy}_2\text{Ti}_2\text{O}_7$ single crystals.

Similar investigations have been done for growing other $R_2\text{Ti}_2\text{O}_7$ crystals and the obtained single crystals are presented in Fig. 3. It was found that $\text{Ho}_2\text{Ti}_2\text{O}_7$ and $\text{Gd}_2\text{Ti}_2\text{O}_7$ could also be grown under 0.4 MPa oxygen pressure while the growth rate is another adjustable parameter, which is important for stabilizing the molten zone [8]. A homogenous

high-quality $\text{Ho}_2\text{Ti}_2\text{O}_7$ crystal could be obtained with a rate of 4 mm/h. A lower speed of 2.5 mm/h was found to be better for growing $\text{Gd}_2\text{Ti}_2\text{O}_7$. On the other hand, the growth rate was found to be less crucial for $\text{Tb}_2\text{Ti}_2\text{O}_7$ under 0.4 MPa oxygen pressure; high-quality crystals were grown with the rate of either 2.5 or 4 mm/h. The situations are a bit different for $\text{Er}_2\text{Ti}_2\text{O}_7$ and $\text{Yb}_2\text{Ti}_2\text{O}_7$, it is found that the crystals grown under high oxygen pressure always have a large number of small cracks even though different growth rates were tried. Very-high-quality single crystals of $\text{Er}_2\text{Ti}_2\text{O}_7$ and $\text{Yb}_2\text{Ti}_2\text{O}_7$ can be grown only under 0.1 MPa oxygen pressure with the rate of 4 and 3 mm/h, respectively. Whereas $\text{Y}_2\text{Ti}_2\text{O}_7$ requires even smaller oxygen pressure and our best conditions for this crystal are in a normal pressure oxygen-argon mixture with the ratio of 4:1 and at a rate of 4 mm/h. The obtained $\text{Y}_2\text{Ti}_2\text{O}_7$ still has some small cracks at the end part, which might be improved by some slight modification of the growth condition. In addition, the single crystal of $\text{Lu}_2\text{Ti}_2\text{O}_7$ was obtained under 0.1 MPa oxygen pressure with rate of 4.5 mm/h, and has a morphology similar to that of $\text{Y}_2\text{Ti}_2\text{O}_7$. Single crystals of $\text{Tb}_{1.8}\text{Y}_{0.2}\text{Ti}_2\text{O}_7$ and TbYTi_2O_7 were successfully obtained under 0.25 MPa oxygen pressure with rates of 2.5 and 3 mm/h, respectively, and have similar appearance to that of $\text{Tb}_2\text{Ti}_2\text{O}_7$. The optimum growth conditions of the $R_2\text{Ti}_2\text{O}_7$ single crystals are included in Table 1. The lattice constants are obtained from the powder X-ray diffraction data and are found to be consistent with the results from the literature [9]. It should be noted that the lattice constants of $R_2\text{Ti}_2\text{O}_7$ have some weak dependencies on the oxygen content [10, 12]. In our case, the lattice constants of the $\text{Tb}_2\text{Ti}_2\text{O}_7$ crystals grown in 0.4 MPa oxygen pressure and annealed in 0.1 MPa oxygen pressure are 10.155(2) and 10.152(1)Å, respectively, which also indicates the weak dependence of lattice constant on oxygen content.

It is worth noting that the quality of $R_2\text{Ti}_2\text{O}_7$ crystals can be easily judged from their appearances. Our subsequent structural and physical-property analyses demonstrated that crystals with good appearances, like shining surface, homogenous color and no cracks, always have high quality. The less successful growths of single crystals with poor appearances were found to have impurity phases. For example, the X-ray diffraction indicated that the single crystal $\text{Dy}_2\text{Ti}_2\text{O}_7$ obtained with a rate of 2 mm/h has a impurity phase of Dy_2TiO_5 .

On the other hand, the color change of the $R_2\text{Ti}_2\text{O}_7$ single crystals could be indicative of slight variation in the oxygen content [12]. As shown in Figs. 1 (a) and 1 (b), the color of $\text{Dy}_2\text{Ti}_2\text{O}_7$ single crystal grown in 0.4 MPa oxygen pressure is deeper than that grown in 0.3 MPa oxygen pressure. Apparently, the crystal with lighter color has smaller oxygen content. A post-annealing confirmed this, that is, the color of $\text{Dy}_2\text{Ti}_2\text{O}_7$ single crystal becomes much lighter after annealing the crystal in normal-pressure O_2 , as shown in Fig. 1 (c). This phenomenon demonstrates that deeper-colored $\text{Dy}_2\text{Ti}_2\text{O}_7$ crystal has larger oxygen content and is more likely free from the oxygen vacancies. Similar phenomenon was also found in other $R_2\text{Ti}_2\text{O}_7$ crystals.

One remarkable problem which has been encountered for the growth of $R_2\text{Ti}_2\text{O}_7$ single crystals is how to avoid small cracks. It has been discussed in previous reports that single crystal was easily to have thermal cracks if a single-crystal seed was used [12]. However, we found that seed bar does not have any influence on the quality of single crystal; in contrast, suitable oxygen pressure and growth rate are more important to reduce the thermal cracks and get good single crystals.

The most important finding in the present work is that the optimum growth conditions are obviously different for different rare-earth titanates. As displayed in Table 1, those compounds with relatively larger radius of R^{3+} ions need to be grown in higher oxygen pressure, like $\text{Gd}_2\text{Ti}_2\text{O}_7$, $\text{Tb}_2\text{Ti}_2\text{O}_7$, $\text{Dy}_2\text{Ti}_2\text{O}_7$, $\text{Ho}_2\text{Ti}_2\text{O}_7$, while those with small radius of R^{3+} ions should be grown under relatively low pressure, such as $\text{Er}_2\text{Ti}_2\text{O}_7$, $\text{Yb}_2\text{Ti}_2\text{O}_7$, $\text{Y}_2\text{Ti}_2\text{O}_7$ and $\text{Lu}_2\text{Ti}_2\text{O}_7$. The growth condition for $\text{Tb}_{1-x}\text{Y}_x\text{Ti}_2\text{O}_7$ single crystals also confirms this law. As we known, pyrochlore oxides are represented by the chemical formula $A_2B_2O_6O'$, where A is a trivalent rare earth consisting of the lanthanides, Y, or Sc, and B could be a transition metal, which is sitting at $16c$ and $16d$ sites of the $Fd\bar{3}m$ space group, respectively. Both A and B form three-dimensional corner-sharing tetrahedra and are coordinated by oxygen ions, and the content of the O' atom plays an important role in the coordination geometry of the A and B sites [1]. In addition, the structure-field or stability-field map for $A_2B_2O_7$ materials show that not only the stability of pyrochlore phase but also the defect concentration are influenced by the radius ratio of A^{3+}/B^{4+} . For instance, the pyrochlore phase

must be synthesized by using high pressure if B ion has very small radius, like Mn^{4+} ion [1]. It is therefore understandable that the oxygen pressure plays a crucial role in the growth of $R_2Ti_2O_7$ crystals and avoiding thermal cracks. One may note that in the present work the oxygen pressure for the optimized growth is larger than those in earlier reports [8, 12]. The main reason why a high oxygen pressure is helpful for growing $R_2Ti_2O_7$ is that it can reduce the evaporation from molten zone and suppress the micro bubbles at the melting interface. Furthermore, a high oxygen pressure could avoid the oxygen deficiency and stabilize the phase formation of $R_2Ti_2O_7$.

3. Magnetic susceptibility and specific heat

Besides the structural characterizations of the obtained $R_2Ti_2O_7$ and $Tb_{2-x}Y_xTi_2O_7$ single crystals using powder X-ray diffraction, single-crystal rocking curve and Laue photograph, the basic physical properties of these crystals were also characterized. DC magnetization and specific heat measurements were done using a SQUID-VSM (Quantum Design) and a Physical Property Measurement System (PPMS, Quantum Design), respectively. In general, both the magnetic susceptibility and specific heat results of our single crystals are consistent with most of data in literatures. Here we show some representative data.

Fig. 4 shows the magnetization curves of $Gd_2Ti_2O_7$ and $Er_2Ti_2O_7$ at 2 K along three characteristic axes [100], [111], and [110]. Since the demagnetization effect is not negligible in this system, the magnetization measurements along three axes are done on samples with similar long-bar shape, of which the size is about $2 \times 0.75 \times 0.75$ mm³. The magnetic field is always applied along the longest dimension, therefore the demagnetization factor is about 0.15 for these samples. $Gd_2Ti_2O_7$ is regarded as a Heisenberg antiferromagnet since Gd^{3+} has no orbital moment. But actually, it exhibits weak anisotropy at low temperatures as shown in Fig. 4(a), which means that other exchange interactions than a simple Heisenberg one should be taken into account [13, 15]. Although the specific heat, neutron scattering and some other experiments indicated that $Er_2Ti_2O_7$ has a strong local XY -type anisotropy [4, 16], there has been no report on the anisotropic magnetization of $Er_2Ti_2O_7$ single crystals. Our magnetization results in Fig. 4(b) show a weak anisotropy of $Er_2Ti_2O_7$ at 2 K. In

addition, the magnetic susceptibilities of $\text{Tb}_2\text{Ti}_2\text{O}_7$ crystals annealed under 0.1 MPa oxygen pressure were measured and compared with that of as-grown crystals. It was found that the magnetism down to 2 K is almost independent of the oxygen content and just shows subtle difference, as shown in Fig. 5 [10].

Low-temperature specific heat data of $R_2\text{Ti}_2\text{O}_7$ ($R = \text{Dy}, \text{Tb}, \text{Gd}, \text{Er}, \text{Yb}, \text{Y}$ and Lu) single crystals are shown in Fig. 6(a). The nonmagnetic $\text{Y}_2\text{Ti}_2\text{O}_7$ and $\text{Lu}_2\text{Ti}_2\text{O}_7$ show a simple behavior of lattice heat capacity. The specific heat of $\text{Dy}_2\text{Ti}_2\text{O}_7$ exhibits a peak around 1 K but does not show any sign of long-range order down to 0.4 K [17]. There is only one broad peak around 2.5 K in the specific-heat data of $\text{Yb}_2\text{Ti}_2\text{O}_7$ with temperature down to 0.4 K [18, 19]. For $\text{Gd}_2\text{Ti}_2\text{O}_7$, there are two sharp peaks at 0.7 and 1 K, which are attributed to the development of long-range magnetic order below about 1 K [13, 14]. The specific heat of $\text{Er}_2\text{Ti}_2\text{O}_7$ also displays a sharp peak at about 1.2 K, corresponding to a second-order phase transition [4, 20]. Two broad peaks at about 0.7 and 6 K are observed in the specific-heat data of $\text{Tb}_2\text{Ti}_2\text{O}_7$. It is fundamentally consistent with previous reports [6, 21, 22, 23], although there are some differences of the data among different samples. The peak at 6 K was attributed to a remnant of an excitation between the ground state doublet and an excited doublet, separated by ~ 18 K, which was related to the short-range magnetic correlation [21, 22]. The peak at 0.7 K was mainly attributed to the splitting of the ground state doublet, and the same short-range magnetic correlation effect also can not be neglected [21, 22].

The partial substituting Tb^{3+} ions with nonmagnetic Y^{3+} ions is naturally expected to have an impact on the low-temperature magnetism of $\text{Tb}_2\text{Ti}_2\text{O}_7$. Fig. 7 shows the temperature dependencies of magnetization with $H \parallel [111]$ and the zero-field specific heat of $\text{Tb}_2\text{Ti}_2\text{O}_7$, $\text{Tb}_{1.8}\text{Y}_{0.2}\text{Ti}_2\text{O}_7$, and TbYTi_2O_7 crystals. It is found that the magnetic properties of $\text{Tb}_{2-x}\text{Y}_x\text{Ti}_2\text{O}_7$ is not a simple combination of the spin liquid $\text{Tb}_2\text{Ti}_2\text{O}_7$ and nonmagnetic material $\text{Y}_2\text{Ti}_2\text{O}_7$. For the Y-doping effect on the specific heat, the magnitudes of the two peaks decrease and the 6 K peak is almost completely suppressed when the Y^{3+} content reaches 50 %, which strongly indicates that the nonmagnetic Y^{3+} doped in $\text{Tb}_2\text{Ti}_2\text{O}_7$ weakens the magnetic interaction of Tb^{3+} . Moreover, the 0.7 K peak moves to higher temperature

with doping, which indicates that the Schottky anomaly related ground state doublet splitting is enlarged by the partial Y^{3+} doping. This could be related to the structural distortions induced by Y doping. In general, the substitution of Y^{3+} ions for Tb^{3+} ions only results in a moderate effect on the magnetism of $Tb_2Ti_2O_7$. These results are essentially consistent with those from Muon spin relaxation and neutron spin echo measurements, which have revealed that Y^{3+} doping slows down the spin fluctuations but the cooperative paramagnetic behavior still persists down to very low temperatures [24].

4. CONCLUSIONS

High quality and large $R_2Ti_2O_7$ ($R = Gd, Tb, Dy, Ho, Y, Er, Yb$ and Lu) and $Tb_{2-x}Y_xTi_2O_7$ ($x = 0.2$ and 1) single crystals were grown by the optical floating-zone method. The growth conditions were optimized and were found to be dependent on the radius of the R^{3+} ions. The structure and crystallinity of single crystals were characterized by X-ray diffraction and Laue photographs. The physical properties were characterized by low-temperature magnetization and specific heat measurements.

ACKNOWLEDGMENTS

This work was supported by the National Natural Science Foundation of China, the National Basic Research Program of China (Grant Nos. 2009CB929502 and 2011CBA00111), and the Fundamental Research Funds for the Central Universities (Program No. WK2340000035).

References

- [1] J. S. Gardner, M. J. P. Gingras, J. E. Greedan, *Rev. Mod. Phys.* **82** (2010) 53.
- [2] J. S. Gardner, S. R. Dunsiger, B. D. Gaulin, M. J. P. Gingras, J. E. Greedan, R. F. Kiefl, M. D. Lumsden, W. A. MacFarlane, N. P. Raju, J. E. Sonier, I. Swainson, Z. Tun, *Phys. Rev. Lett.* **82** (1999) 1012.
- [3] A. P. Ramirez, A. Hayashi, R. J. Cava, R. Siddharthan, B. S. Shastry, *Nature* **399** (1999) 333.
- [4] J. P. C. Ruff, J. P. Clancy, A. Bourque, M. A. White, M. Ramazanoglu, J. S. Gardner, Y. Qiu, J. R. D. Copley, M. B. Johnson, H. A. Dabkowska, B. D. Gaulin, *Phys. Rev. Lett.* **101** (2008) 147205 .
- [5] L. J. Chang, S. Onoda, Y. Su, Y. J. Kao, K. D. Tsuei, Y. Yasui, K. Kakurai, M. R. Lees, *Nat. Commun.* **3** (2012) 992.

- [6] H. Takatsu, H. Kadowaki, T. J. Sato, J. W. Lynn, Y. Tabata, T. Yamazaki, K. Matsuhira, *J. Phys.: Condens. Matter* **24** (2012) 052021.
- [7] B. Wanklyn, *J. Mater. Sci.* **3** (1968) 395.
- [8] G. Balakrishnan, O. A. Petrenko, M. R. Lees, D. McK. Paul, *J. Phys.: Condens. Matter* **10** (1998) 723.
- [9] J. Lian, J. Chen, L. M. Wang, R. C. Ewing, J. M. Farmer, L. A. Boatner, K. B. Helean, *Phys. Rev. B* **68** (2003) 134107 .
- [10] J. S. Gardner, B. D. Gaulin, D. McK. Paul, *J. Cryst. Growth* **191** (1998) 740.
- [11] M. B. Johnson, D. D. James, A. Bourque, H. A. Dabkowska, B. D. Gaulin, M. A. White, *J. Solid State Chem.* **182** (2009) 725.
- [12] D. Prabhakaran A. T. Boothroyd, *J. Cryst. Growth* **318** (2011) 1053.
- [13] O. A. Petrenko, M. R. Lees, G. Balakrishnan, D. McK. Paul, *Phys. Rev. B* **70** (2004) 012402.
- [14] A. Yaouanc, P. Dalmas de Réotier, V. Glazkov, C. Marin, P. Bonville, J. A. Hodges, P. C. M. Gubbens, S. Sakarya, C. Baines, *Phys. Rev. Lett.* **95** (2005) 047203.
- [15] P. Bonville, J. A. Hodges, M. Ocio, J. P. Sanchez, P. Vulliet, S. Sosin, D. Braithwaite, *J. Phys.: Condens. Matter* **15** (2003) 7777.
- [16] O. A. Petrenko, M. R. Lees, G. Balakrishnan, *J. Phys.: Condens. Matter* **23** (2011) 164218.
- [17] Z. Hiroi, K. Matsuhira, S. Takagi, T. Tayama, T. Sakakibara, *J. Phys. Soc. Jpn.* **72** (2003) 411.
- [18] H. Blöte, R. Wielinga, W. Huiskamp, *Physica* **43**, 549 (1969).
- [19] A. Yaouanc, P. Dalmas de Réotier, C. Marin, V. Glazkov, *Phys. Rev. B* **84** (2011) 172408.
- [20] P. Dalmas de Réotier, A. Yaouanc, Y. Chapuis, S. H. Curnoe, B. Grenier, E. Ressouche, C. Marin, J. Lago, C. Baines, S. R. Giblin *Phys. Rev. B* **86** (2012) 104424.
- [21] M. J. P. Gingras, B. C. den Hertog, M. Faucher, J. S. Gardner, S. R. Dunsiger, L. J. Chang, B. D. Gaulin, N. P. Raju, J. E. Greedan, *Phys. Rev. B* **62** (2000) 6496.
- [22] N. Hamaguchi, T. Matsushita, N. Wada, Y. Yasui, M. Sato, *Phys. Rev. B* **69** (2004) 132413.
- [23] A. Yaouanc, P. Dalmas de Réotier, Y. Chapuis, C. Marin, S. Vanishri, D. Aoki, B. Fåk, L.-P. Regnault, C. Buisson, A. Amato, C. Baines, A. D. Hillier, *Phys. Rev. B* **84** (2011) 184403.
- [24] A. Keren, J. S. Gardner, G. Ehlers, A. Fukaya, E. Segal, Y. J. Uemura, *Phys. Rev. Lett.* **92** (2004) 107204.

Figure 1: (Color online) Single crystals of $\text{Dy}_2\text{Ti}_2\text{O}_7$ grown at 2.5 mm/h under 0.3 MPa O_2 pressure (a) and at 4 mm/h under 0.4 MPa O_2 pressure (b), respectively. (c) Single crystal shown in panel (b) after annealing at 900°C in normal-pressure O_2 .

Figure 2: X-ray diffraction pattern of (110) plane (a) and the rocking curve of (440) peak (b) for a piece of $\text{Dy}_2\text{Ti}_2\text{O}_7$ crystal, which was orientated by using the X-ray Laue photographs.

Figure 3: (Color online) Single crystals of $\text{Ho}_2\text{Ti}_2\text{O}_7$ (a), $\text{Tb}_2\text{Ti}_2\text{O}_7$ (b), and $\text{Gd}_2\text{Ti}_2\text{O}_7$ (c) grown under 0.4 MPa O_2 pressure at rates of 4 mm/h, 4 mm/h, and 2.5 mm/h, respectively. Single crystals of $\text{Er}_2\text{Ti}_2\text{O}_7$ (d) and $\text{Yb}_2\text{Ti}_2\text{O}_7$ (e) grown under 0.1 MPa O_2 pressure at rates of 4 mm/h and 3 mm/h, respectively. (f) Single crystal of $\text{Y}_2\text{Ti}_2\text{O}_7$ grown at 4 mm/h in O_2 and Ar mixture with the ratio of 4:1.

Figure 4: (Color online) Magnetization curves of $\text{Gd}_2\text{Ti}_2\text{O}_7$ (a) and $\text{Er}_2\text{Ti}_2\text{O}_7$ (b) single crystals with magnetic field along the [100], [111], and [110] axes at 2 K. The demagnetization field is not corrected.

Figure 5: (Color online) Magnetic susceptibilities of one $\text{Tb}_2\text{Ti}_2\text{O}_7$ single crystal before and after annealed in 0,1 MPa O_2 . The magnetic fields are applied along the [110] axe. Inset: the magntizations curves at 2 K.

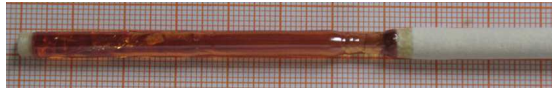
Figure 6: (Color online) Temperature dependencies of specific heat of $R_2\text{Ti}_2\text{O}_7$ ($R = \text{Dy}, \text{Tb}, \text{Gd}, \text{Er}, \text{Yb}, \text{Y}$ and Lu) single crystals in zero field.

Figure 7: (Color online) Temperature dependencies of magnetization with magnetic field along the [111] axes (a) and the specific heat (b) of $\text{Tb}_2\text{Ti}_2\text{O}_7$, $\text{Tb}_{1.8}\text{Y}_{0.2}\text{Ti}_2\text{O}_7$, and TbYTi_2O_7 single crystals. The data is calculated with per mole of formula unit.

Fig. 1

a

$\text{Dy}_2\text{Ti}_2\text{O}_7$



2.5 mm/h 0.3MPa

b



4 mm/h 0.4MPa

c



Annealed in O₂

Fig. 2

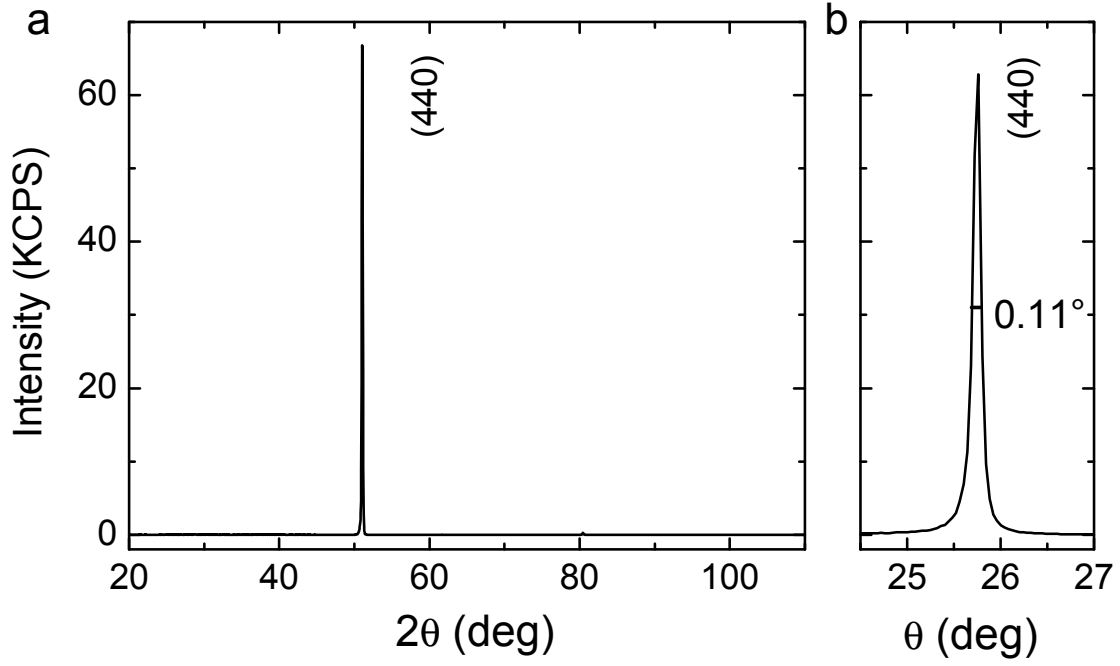


Fig. 3

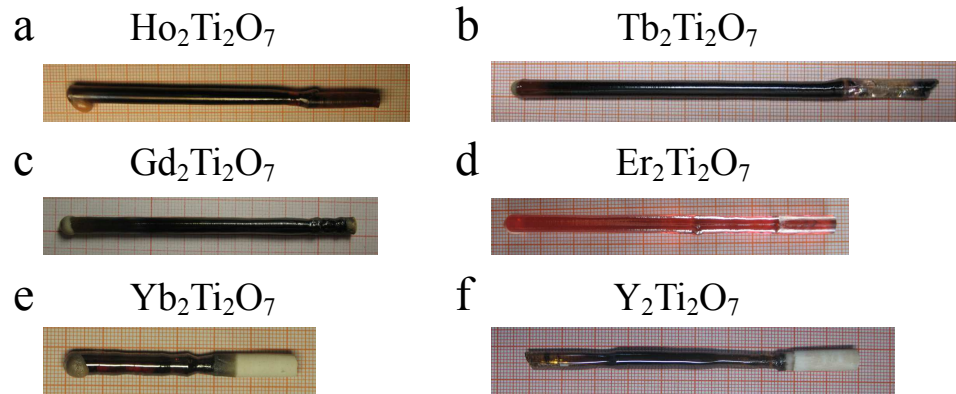


Table 1: Optimized growth conditions for different rare-earth titanates. The lattice parameters are obtained from the powder X-ray diffraction of single crystals.

	R ³⁺ radius (Å)	Lattice parameter (Å)	Growth rate (mm/h)	Atomosphere
Gd ₂ Ti ₂ O ₇	0.94	10.196(9)	2.5	0.4 MPa O ₂
Tb ₂ Ti ₂ O ₇	0.92	10.155(2)	2.5, 4	0.4 MPa O ₂
Dy ₂ Ti ₂ O ₇	0.91	10.127(5)	4	0.4 MPa O ₂
Ho ₂ Ti ₂ O ₇	0.89	10.105(2)	4	0.4 MPa O ₂
Y ₂ Ti ₂ O ₇	0.89	10.089(3)	4	0.1 MPa O ₂ +Ar(4:1)
Er ₂ Ti ₂ O ₇	0.88	10.072(3)	4	0.1 MPa O ₂
Yb ₂ Ti ₂ O ₇	0.88	10.033(2)	3	0.1 MPa O ₂

Fig. 4

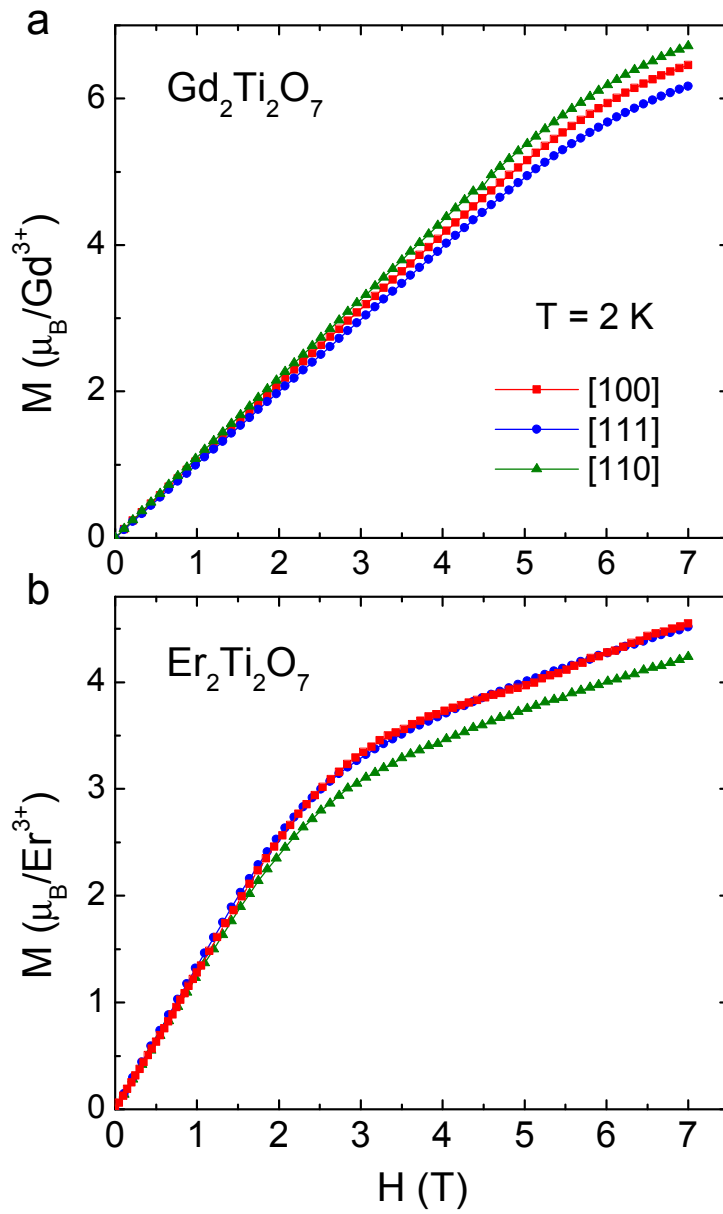


Fig. 5

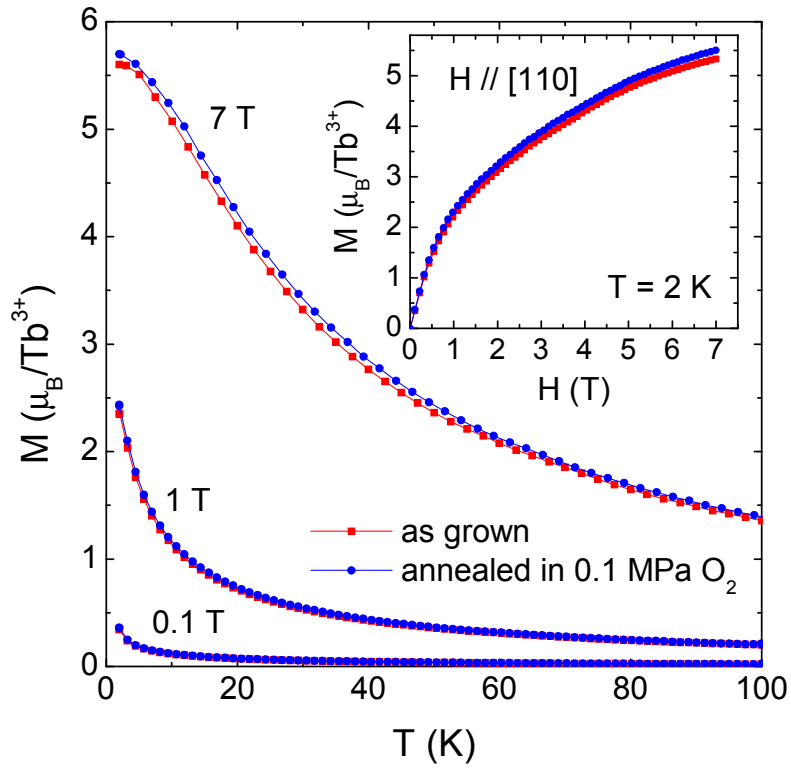


Fig. 6

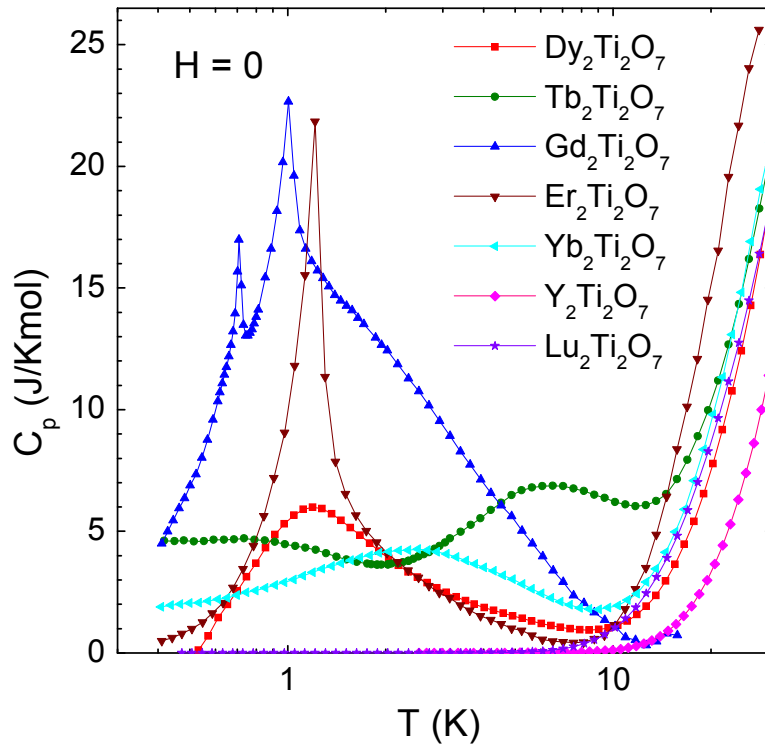


Fig. 7

